Microstructures of Conventionally As-Cast Mg–Zn–Y Alloys

Qian Li, Zhenghua Huang, Yongxin Zhou, Chunjie Xu, Yangde Li and Weirong Li

Abstract Two series ingots of $Mg_{69+x}Zn_{30-x}Y_1$ and $Mg_{68+x}Zn_{30-x}Y_2$ (x = 0, 3 and 6, atomic percent) alloys with the diameter of 100 mm were obtained by ordinary gravity casting, respectively. The phase compositions and microstructures were investigated by means of optical microscope (OM), scanning electron microscopy (SEM) and X-ray diffraction (XRD). The law that the number, morphology, size and distribution of the quasicrystal phase varied with the content of Zn and Y was discussed. The results showed that the microstructures of the two series alloys were composed of MgZn matrix, $Mg_{30}Zn_{60}Y_{10}$ quasicrystal phase (I) and α-Mg phase. The I-phase directly nucleated and grew during the cooling process of Mg–Zn–Y melt. The morphology of the two series alloys was different obviously. The I-phase exhibited small pentagonal or five-petal shape and six-petal shape in the microstructure of the $Mg_{69+x}Zn_{30-x}Y_1$ alloy, while it was not regular polygon shape in the microstructure of the $Mg_{68+x}Zn_{30-x}Y_2$ alloy. At the same time,

Q. Li · Z. Huang (✉)
Guangdong Provincial Key Laboratory for Technology and Application of Metal Toughening, Guangdong Institute of Materials and Processing, Guangzhou 510650, China
e-mail: zhhuang@live.cn

Q. Li
e-mail: 240008439@qq.com

Q. Li · Y. Zhou · C. Xu
School of Materials Science and Engineering, Xi'an University of Technology, Xi'an 710048, China
e-mail: zhouyongxin_88@126.com

C. Xu
e-mail: xuchunjie@gmail.com

Y. Li · W. Li
DongGuan EONTEC Co., Ltd, DongGuan 523662, China
e-mail: patent@e-ande.com

W. Li
e-mail: patent@e-ande.com

Y. Han (ed.), *Advances in Materials Processing*, Lecture Notes in Mechanical Engineering, https://doi.org/10.1007/978-981-13-0107-0_54

with decreasing Zn content, the granularity and homogenization degree of the quasicrystals enhanced gradually. The quasicrystals increased and distributed more evenly.

Keywords Mg–Zn–Y alloy · Quasicrystal · Icosahedral · Alloy composition

Introduction

As the lightest structural metal material, the prospect of magnesium alloys is promising. However, it seems rather difficult to design Mg-based alloy due to lack of effective reinforcement. Mg–Zn series alloys can enhance alloy strength sharply by aging strengthening. The further addition of rare earth RE, being the most effective way to produce the reinforcement effect by second phase, can form large numbers of compounds with high thermal stability [1]. So far, there has been a considerable amount of Mg alloys that have been developed for the enhancement of icosahedral quasicrystal phase (I-phase). They found that the second phase of as-cast Mg–Zn–Y alloy was mainly I-phase when atomic ratio of Zn: RE was about 6. I-phase with the non-periodic arrangement of atoms exhibits high hardness, low interface and strong I-phase/Mg interface, so it can be used as an efficient reinforcing phase for Mg alloy [2–6]. The discovery of quasicrystalline phase in Mg–Zn–Y alloy becomes a new research direction for developing Mg alloys with high performance [7]. The influence of different composition proportion on the solidification phase and microstructure of Mg–Zn–Y alloy had been studied [8]. However, the effect of the Zn and Y contents on quasicrystalline phase in Mg–Zn–Y alloy was rarely reported. Therefore, the present paper is focused on studying the microstructures of as-cast $Mg_{69+x}Zn_{30-x}Y_1$ alloys and $Mg_{68+x}Zn_{30-x}Y_2$ alloys and discussing the relation between the number, morphology, size and distribution of the quasicrystal phase and the Zn and Y contents. Then, it can provide the basis for controlling the microstructure and designing the composition of Mg alloys.

Experimental

The alloy ingots were prepared with industrial pure Mg, pure Zn and Mg–31.7%Y (mass fraction) master alloy in a melting furnace under a mixed CO_2 and SF_6 protective atmosphere. The nominal components are listed in Table 1. Pure Zn and master alloy were added in turn when pure Mg was melted and heated up to 973 K. The melt was stirred twice within 1 h and refined. Then the melt was heated up to 1003 K and stewed for 30 min. When the temperature of the melt cooled down to 973 K, the melt was poured into the round metal mould with the preheating temperature of 473 K, and then the as-cast samples were obtained.

Table 1 Mass ratio of each element of experimental alloys

Alloy	Mg [wt%]	Zn [wt%]	Y [wt%]
$Mg_{69}Zn_{30}Y_1$	44.99	52.63	2.38
$Mg_{72}Zn_{27}Y_1$	48.55	48.98	2.47
$Mg_{75}Zn_{24}Y_1$	52.36	45.08	2.56
$Mg_{68}Zn_{30}Y_2$	43.58	51.73	4.69
$Mg_{71}Zn_{27}Y_2$	47.03	48.12	4.85
$Mg_{74}Zn_{24}Y_2$	50.72	44.26	5.02

As-cast specimens were made as metallographic specimen after being corroded with 4% HNO_3 (volume fraction) in ethanol. Then the microstructure were observed on optical microscope (OM, Leica DM IRM) and scanning electron microscope (SEM, JEOL JXA-8100). The phase composition analysis was performed on X-ray diffractometer (XRD, SmartLab) with Cu K_α radiation.

Results and Discussion

Figures 1 and 2 show the OM and SEM graphs of as-cast $Mg_{69+x}Zn_{30-x}Y_1$ alloys, respectively. Combined with the XRD pattern (Fig. 3a), the microstructure of as-cast $Mg_{69}Zn_{30}Y_1$ alloy includes gray MgZn matrix, and incompletely grown pentagonal, five and six petals-like $Mg_{30}Zn_{60}Y_{10}$ (I-phase). It can be seen from Fig. 1f that I-phase usually exhibits a pentagonal "flower core" and "petal type" dendritic like crystal, which grows outward and is known as "primary petal" of quasicrystal. A "burr" protruding from the edge of primary petal, which is similar to secondary axis of dendrite, is known as "secondary petal" of quasicrystal. With decreasing the Zn content to 27%, the block or tree-like α-Mg solid solution precipiates. At the same time, the incompletely grown pentagonal phase decreases and the petals-like I-phase increases. When the Zn content further decreases to 24%, I-phase grows, and the five and six petals-like I-phase increases significantly. Meanwhile, few laminar eutectic (I-phase + α-Mg) appears.

As a result, the size, quantity and distribution of quasicrystal particles in $Mg_{69+x}Zn_{30-x}Y_1$ alloys change significantly with the alloy composition. With decreasing the Zn content, the granularity and homogenization degree of quasicrystal increase. At the same time, the I-phase increases and distributes more uniformly.

Figures 4 and 5 show the OM and SEM graphs of as-cast $Mg_{68+x}Zn_{30-x}Y_2$ alloys, respectively. Combined with its XRD pattern (see Fig. 3b), the microstructure of as-cast $Mg_{68}Zn_{30}Y_2$ alloy includes gray MgZn matrix, ruleless and polygonal I-phase, α-Mg solid solution with black particles and few laminar eutectic (I-phase + α-Mg).

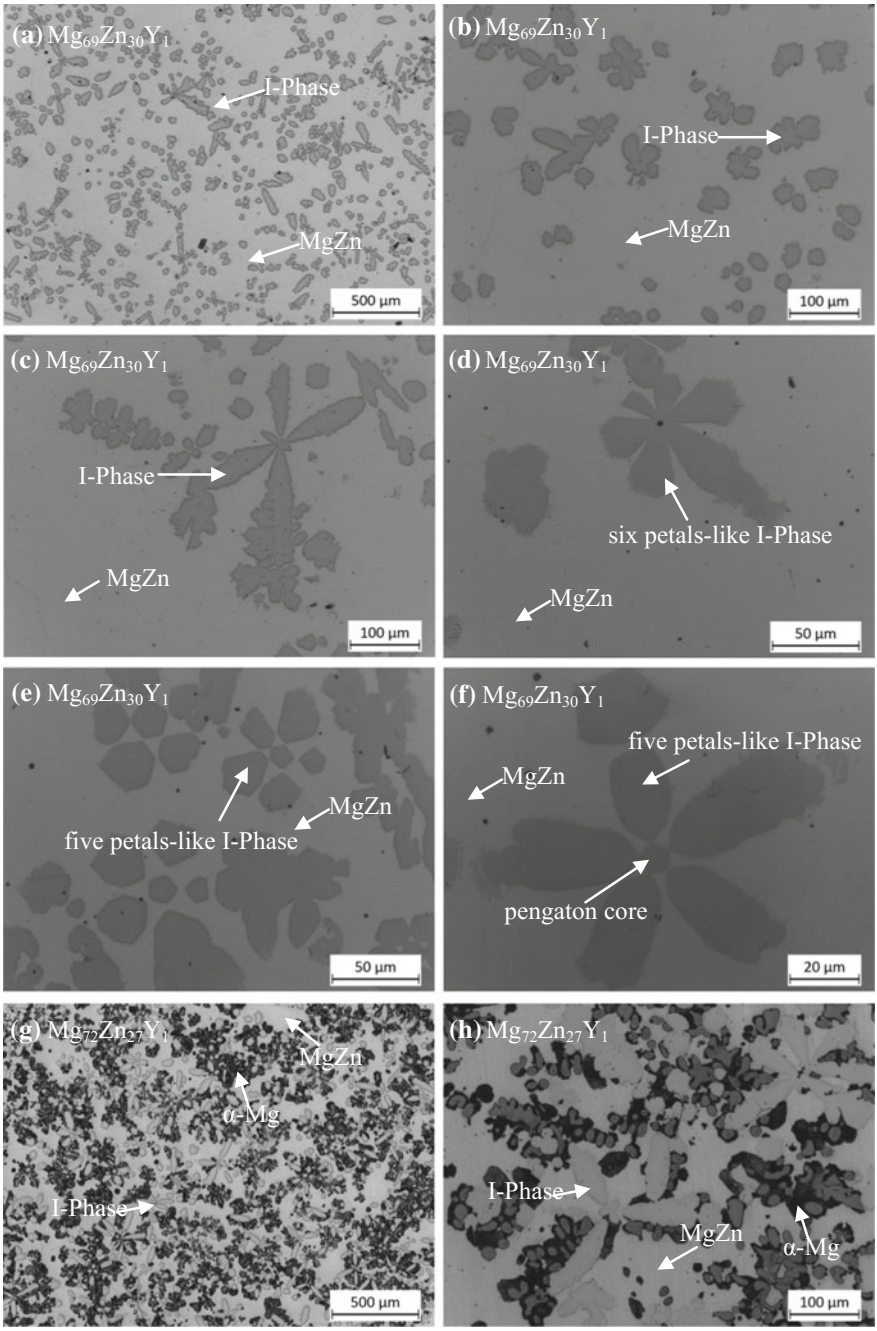

Fig. 1 OM graphs of as-cast $Mg_{69+x}Zn_{30-x}Y_1$ alloys

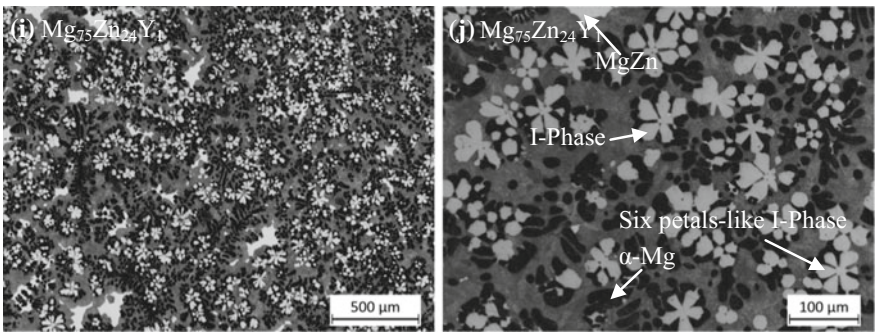

Fig. 1 (continued)

With decreasing the Zn content to 27%, the ruleless and polygonal I-phase decreases and the laminar eutectic (I-phase + α-Mg) increases. When the Zn content further decrease to 24%, the ruleless and polygonal I-phase decreases significantly and the size of I-phase particles also decreases. Meanwhile, the laminar eutectic (I-phase + α-Mg) continuously increases.

Compared with $Mg_{69+x}Zn_{30-x}Y_1$ alloys, the microstructures of $Mg_{68+x}Zn_{30-x}Y_2$ alloys change significantly due to the increase in the Y content. The quasicrystalline phase mainly exists as incompletely grown pentagon, five and six petals for $Mg_{69+x}Zn_{30-x}Y_1$ alloys, while it does in the form of ruleless and polygonal I-phase and laminar eutectic (I-phase + α-Mg) for $Mg_{68+x}Zn_{30-x}Y_2$ alloys.

Despite the fact that the quasicrystalline phase exists in microstructure alloy by specific morphology and exhibits different orientation, its formation process also follows nucleation and growth law. According to reference [9], the eutectic reaction occurs at 823 K when high temperature melt solidifies:

$$L \rightarrow \alpha\text{-}Mg + Mg_3Zn_3Y_2 \tag{1}$$

$Mg_3Zn_3Y_2$ is W phase. With decreasing the temperature, peritectic reaction occurs at 721 K:

$$L + W \rightarrow \alpha\text{-}Mg + I\text{ - phase} \tag{2}$$

With further decreasing the melt temperature, the eutectic reaction generates Mg_7Zn_3 phase at 613 K:

$$L \rightarrow \alpha\text{-}Mg + Mg_7Zn_3 \tag{3}$$

Finally, eutectoid reaction, which occurs at 598 K, produces MgZn phase:

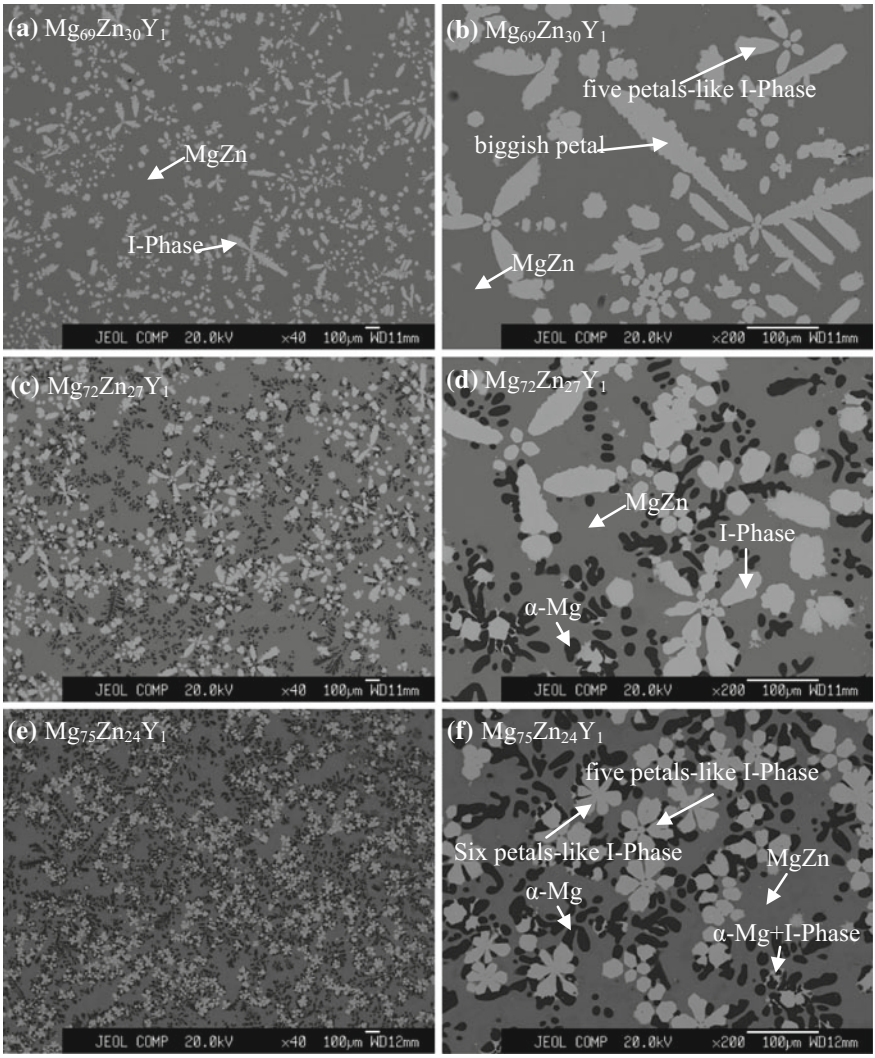

Fig. 2 SEM graphs of as-cast $Mg_{69+x}Zn_{30-x}Y_1$ alloys

$$Mg_7Zn_3 \rightarrow \alpha\text{-}Mg + MgZn \tag{4}$$

In the end, α-Mg solid solution, MgZn matrix and I-phase form, which is consistent with the present results.

The characteristic that crystal nucleus produces stable or metastable phase is to overcome activation energy ΔG^* [10]. According to the classical nucleation theory, each phase ΔG^* expressions can be written as:

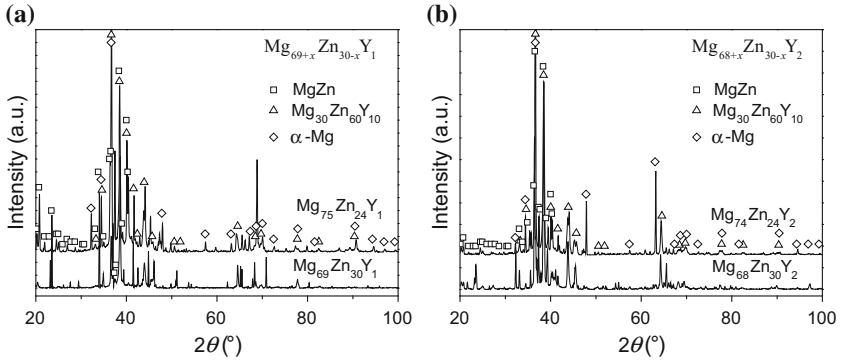

Fig. 3 XRD patterns of as-cast $Mg_{69+x}Zn_{30-x}Y_1$ and $Mg_{68+x}Zn_{30-x}Y_2$ alloys

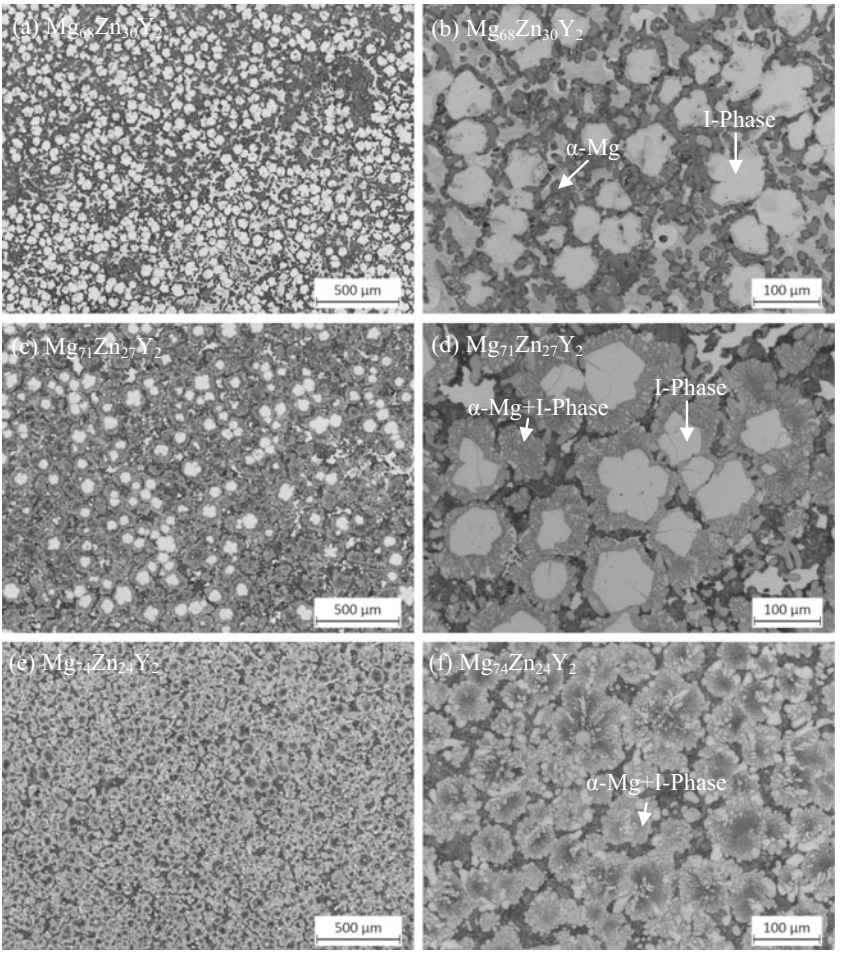

Fig. 4 OM graphs of as-cast $Mg_{68+x}Zn_{30-x}Y_2$ alloys

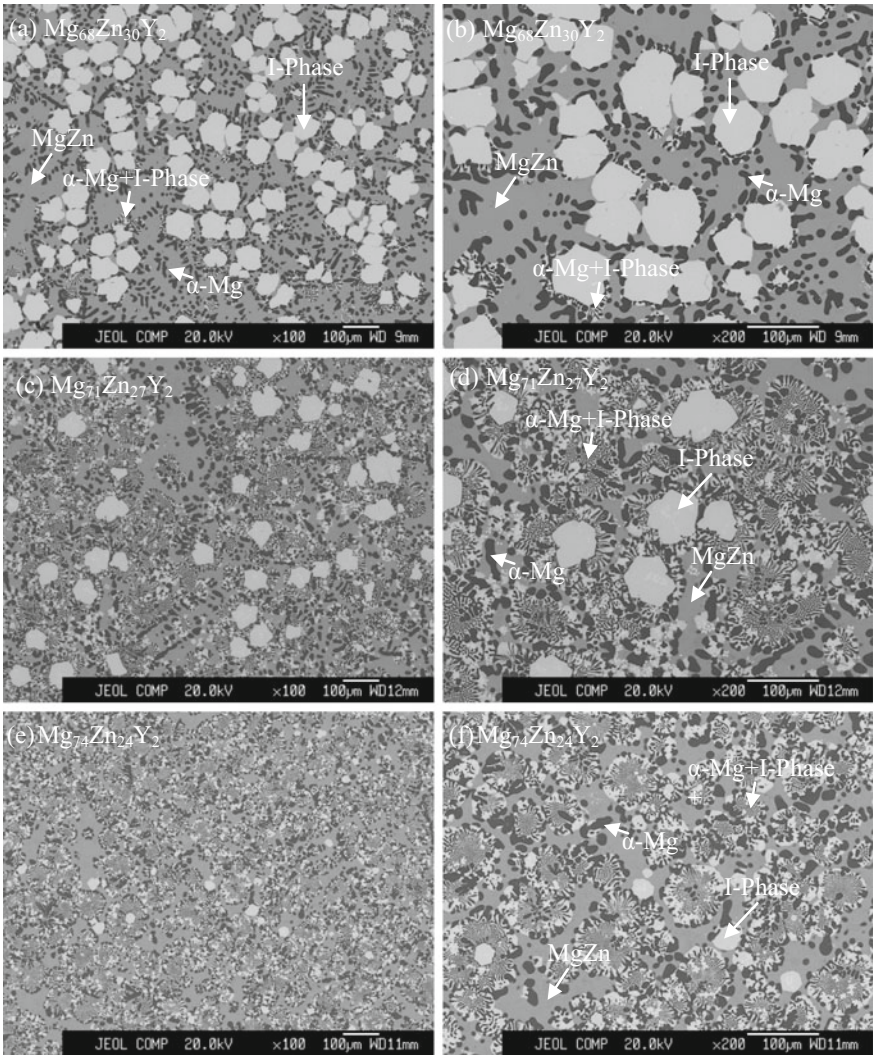

Fig. 5 SEM graphs of as-cast $Mg_{68+x}Zn_{30-x}Y_2$ alloys

$$\Delta G^* = \frac{16\,\sigma_{sl}^3}{3\Delta G^2} f(\theta) \tag{5}$$

where, ΔG is free energy difference between solid and liquid, σ_{sl} is solid-liquid interfacial energy, and $f(\theta)$ is contact angle factor. For homogeneous nuclear systems, $f(\theta) = 1$. ΔG^* consists of two parts: one is ΔG, which is phase-change driving forces, and the other is σ_{sl}, which is phase-change resistance. According to the Spaepen model [11]:

$$\sigma_{sl} = \alpha_s \frac{\Delta S_f}{\left(N_A V_m^2\right)^{1/3}} T \tag{6}$$

where, ΔS_f is melting entropy, N_A is Avogadro constant, V_m is molar volume, T is temperature, and α_s is the parameter associated with the nucleation structure. And for the icosahedral structure and the fcc structure, the value of α_s is 0.36 and 0.86, respectively. It can be seen from Eq. 5 that activation energy ΔG^* is directly proportional to nucleation barrier and directly affects the difficulty of melt nucleation through the size of the nucleation barrier. Therefore, nucleation barrier plays an important role in nucleation process. It can be seen from Eq. 6 that for a certain undercooling temperature, the nucleation barrier depends on the type of crystal structure. As a result, if the crystal structure is similar to the short range order in the melt, the nucleation barrier is lower, which is more favorable for the nucleation of quasicrystalline phase.

According to the morphology, distribution and composition segregation of quasicrystals, it is concluded that quasicrystal formation is quite different from the continuous phase-change of amorphous formation. Similar to the solidification process of crystalline alloys, it follows the nucleation and growth law. In the discussion of the formation mechanism of quasicrystalline phase, it is mentioned that peritectic reaction occurs at 721 K in W phase formed by the eutectic reaction during the solidification process of the melt. At this point, the quasicrystalline phase begins to nucleate and then grows.

The quasicrystal structure has fivefold, threefold and twofold rotational symmetry, whose point group symbol is $m\bar{3}\bar{5}$, and does not belong to any of the 32 crystal point groups. The regular icosahedron contains 12 vertices, each of which is a fivefold axis of rotational symmetry and is 63.43° from the next 5 vertices. If the fastest growth is along 12 vertices, the star shaped grains are obtained. The fivefold symmetrical growth morphologies of the quasicrystal which is made under general solidification reflects and depends on the peculiarity of quasicrystal structure.

The nucleation and growth process of five and six petals-like quasicrystals are explained as follows.

Quasicrystalline phase overcomes the nucleation barrier and grows slowly into a pentagon by peritectic reaction in the permission of nucleation and growth conditions in the liquid alloy (see Fig. 6a). An approximately regular pentagon with five apex angles rapidly grows outward and eventually forms a five-sided petal shape. From the view of morphology of quasicrystal, it may have different growth patterns. First, pentagonal quasicrystal grows into a five petals-like quasicrystal without a flower core, that is, the path from a to b in Fig. 6. Second, pentagonal quasicrystal grows into a five petals-like quasicrystal with a flower core, that is, the path from a to c in Fig. 6. Third, Fig. 6b may also be a transition phase of Fig. 6c. The five vertices of the pentagonal quasicrystal of Fig. 6a extend rapidly toward the alloy liquid, which is shown in Fig. 6b, and then grows into a five petals-like quasicrystalline phase with a flower core, as shown in Fig. 6c.

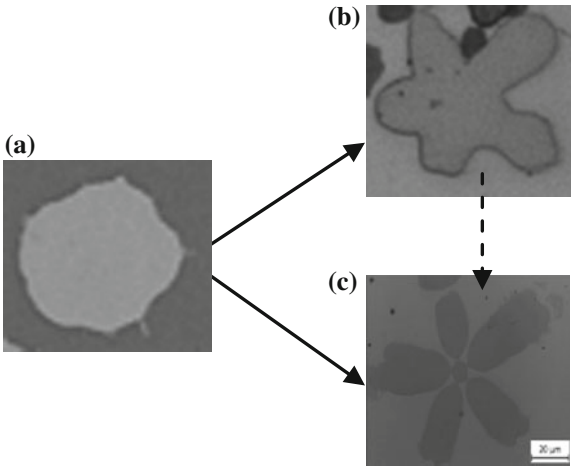

Fig. 6 Schematic diagram of nucleation and growth process of five petals-like quasicrystalline phase

From the formation process, the formation of six petals-like quasicrystal by specific morphology follows the nucleation and growth law. It can be seen from Fig. 7a, b that the embryos grow outwards along six vertices of each other at 60° after the nucleation of quasicrystal. The origin of these six vertices is likely to be the deformation of two-dimensional nucleus or the morphology of I-phase along different sections. However, it can be seen from Fig. 7c that when the six vertices grow to some extent, the three of them which are 120° each other grow rapidly. Then, three other dendrites, each of which are 120°, grow into the melt, as shown in Fig. 7d. The final morphology of the solidification presents six petals-like quasicrystalline phase with different sizes. Compared with five angles, five petals-like and six petals-like quasicrystals, the secondary petal of six petals-like quasicrystals is more developed, as shown in Fig. 7f1, f2. The developed "secondary petal" grows with no direction at the edge of "primary petal".

Figures 1, 2, 4 and 5 show that the morphology of quasicrystalline phase is diverse, which can be divided into the following two categories. (1) Polygon and

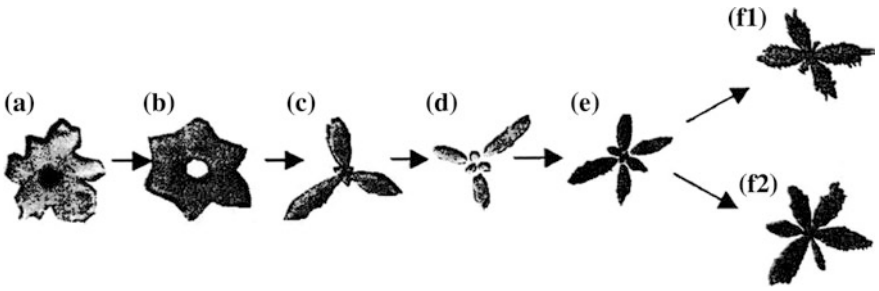

Fig. 7 Schematic diagram of nucleation and growth process of six petals-like quasicrystalline phase [12]

petal-like particles. Some of the quasicrystalline phases have flat and regular geometric shapes, showing the characteristic of faceted growth. And the surface of some quasicrystalline phases is more smooth, showing the characteristic of non faceted growth. (2) Laminar eutectic. Figures 4 and 5 show that the quasicrystalline phase in some alloys exists in the form of laminar eutectic, showing the characteristic of coupled growth.

Under certain conditions, crystals may form polyhedron shapes corresponding to their symmetry. The surfaces of these polyhedra tend to be the lowest in surface energy, or their direction of normal line grows at the slowest rate.

Figure 1e shows a five petals-like quasicrystalline phase with a pentagonal core, and each petal exhibits an obvious pentagonal shape. It can be seen that the petals of the pentagon correspond to the five vertices of the pentagon. And it shows the characteristic of faceted growth. The best growth direction of I-phase is fivefold axis, followed by threefold axis. And the growth speed of twofold axis direction is the slowest [13]. The direction of the center of icosahedral toward vertice is the fivefold axis. Therefore, the optimum growth direction of I-phase is continued to grow at the vertice of I-phase. It can be concluded that the core of petal-like quasicrystalline phase is icosahedral. As the projection of the two-dimensional surface, the direction of the five vertices of the core is fivefold axis direction of I-phase, which is the optimum growth direction of the quasicrystalline phase. In this direction, five petals-like I-phase are grown in faceted growth. And the two-dimensional projection represents five petals-like with a pentagonal core.

As shown in Fig. 1f, the quasicrystalline phase also represents five petals-like with a pentagonal core. It can be seen that the end of the flower petal is round, showing the characteristic of non faceted growth. But the tip of the petals is still flat, indicating that the petals are still growing in faceted growth at the initial stage of growth. With the decrease in the melt temperature, the petals grow further and develop gradually toward non faceted growth patterns. This can be explained by the fact that the driving force of crystal growth has a great influence on the mode of interface growth in accordance with the kinetic theory of crystal growth.

The driving force of crystal growth can be expressed as [14]:

$$\Delta G_{\mathrm{m}} = \frac{\Delta H_0}{T_{\mathrm{m}}} \Delta T_{\mathrm{k}} \tag{7}$$

where, ΔH_0 is latent heat of crystallization and ΔT_{k} is kinetic undercooling of crystals growing up.

Figure 8 shows that the variation of the driving force of crystal growth leads to the transition of crystal growth from discontinuous faceted growth to continuous non faceted growth. The figure is divided into two regions. Area A is a discontinuous faceted growth area, where the smooth faceted interface remains smooth in the range of driving force shown in this region. With the decrease in the melt temperature, the undercooling increases gradually. Equation 7 shows that the driving force of crystal growth increases and reaches Area B. In Area B, the original interface structure becomes unstable. So the smooth faceted interface changes into

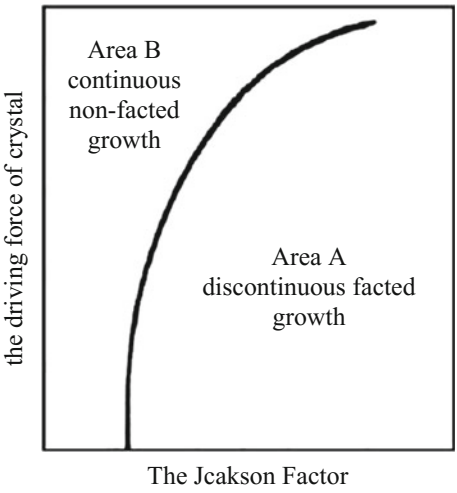

Fig. 8 Variation with driving force of the transition from faceted to continuous growth [15]

rough non-faceted interface. The growth mechanism also translates from discontinuous growth to continuous growth.

In the early stage of solidification, the grain size of the quasicrystal is smaller, which appears to be blocky or globular. With the decrease in the melt temperature, the primary phase in the melt will further grow up. When the primary phase grows and exceeds a critical size, growth will become unstable. The surface inevitably produces some tiny protuberances. These protuberances will continue to grow preferentially and form stable branching, and finally form six petals-like quasicrystalline phase (see Fig. 7). Six petals consist of petals opposing to each other in three opposite directions. In I-phase, only fivefold and threefold axises are opposite axes. The projection of the vertices of icosahedral on the two-dimensional surface in the direction of the threefold axis is exactly six points. And the corresponding directions of the six points are in the direction of the fivefold axis, which is the optimum growth direction of icosahedral.

In a word, quasicrystalline phase has many growth modes, such as faceted growth, non-faceted growth, faceted growth mixing up with non-faceted growth, and coupled growth. From Figs. 1, 2, 4 and 5, it is found that the content of alloying element plays a certain influence on the growth of quasicrystalline phase. With decreasing the Zn content in $Mg_{69+x}Zn_{30-x}Y_1$ alloys, the growth of quasicrystalline phase gradually translates from faceted growth to non faceted growth, and the morphology does from incompletely grown pentagon to five petals and six petals. With decreasing the Zn content in $Mg_{68+x}Zn_{30-x}Y_2$ alloys, the growth of quasicrystalline phase gradually translates from faceted growth to coupled growth.

Summary

The microstructure of as-cast $Mg_{69+x}Zn_{30-x}Y_1$ alloys includes gray MgZn matrix, incompletely grown pentagonal, five and six petals-like $Mg_{30}Zn_{60}Y_{10}$ (I-phase), and few laminar eutectic (I-phase + α-Mg). The microstructure of as-cast $Mg_{68+x}Zn_{30-x}Y_2$ alloys includes gray MgZn matrix, ruleless and polygonal I-phase, α-Mg solid solution with black particles and laminar eutectic. With decreasing the Zn content in $Mg_{69+x}Zn_{30-x}Y_1$ alloys, the growth of quasicrystalline phase gradually translates from faceted growth to non-faceted growth, and the incompletely grown pentagonal phase decreases and the petals-like I-phase increases. With decreasing Zn content in $Mg_{68+x}Zn_{30-x}Y_2$ alloys, the growth of quasicrystalline phase gradually translates from faceted growth to coupled growth, and the ruleless and polygonal I-phase decreases while the laminar eutectic increases.

Acknowledgements This work was supported by Natural Science Foundation of Guangdong Province (2016A030313802), Project on Scientific Research of Guangzhou City (201707010393) and Technology Innovation Project of Science and Technology Small and Medium Enterprise of Guangdong Province (2016A010120024).

References

1. I.J. Polmear, Magnesium alloys and applications. Mater. Sci. Technol. **10**, 1–16 (1994)
2. J.F. Nie, B.C. Muddle, Precipitation in magnesium alloy WE54 during isothermal ageing at 250 °C. Scripta Mater. **40**, 1089–1094 (1999)
3. C. Antion, P. Donnadieu, F. Perrard, A. Deschamps, C. Tassin, A. Pisch, Hardening precipitation in a Mg–4Y–3RE alloy. Acta Mater. **51**, 5335–5348 (2003)
4. D.H. Bae, M.H. Lee, K.T. Kim, W.T. Kim, D.H. Kim, Application of quasicrystalline particles as a strengthening phase in Mg–Zn–Y alloys. J. Alloys Compd. **342**, 445–450 (2002)
5. P.W. Stephens, A.I. Goldman, Metallic phase with long-range orientational order and no translational symmetry. Phys. Rev. Lett. **53**, 1951–1954 (1984)
6. J.S. Zhang, Y.Q. Zhang, Y. Zhang, C.X. Xu, X.M. Wang, J. Yan, Effect of Mg-based spherical quasicrystal on microstructures and mechanical properties of ZA54 alloy. Trans. Nonferrous Met. Soc. Chin. **20**, 1199–1204 (2010)
7. A.I. Goldman, Magnetism in icosahedral quasicrystals: current status and open questions. Sci. Technol. Adv. Mater. **15**, 044801-1–044801-15 (2014)
8. Y.L. Ju, D.H. Kim, H.K. Lim, D.H. Kim, Effects of Zn/Y ratio on microstructure and mechanical properties of Mg-Zn-Y alloys. Mater. Lett. **59**, 3801–3805 (2005)
9. A. Singh, M. Watanabe, A. Kato, A.P. Tsai, Crystallographic orientations and interfaces of icosahedral quasicrystalline phase growing on cubic W phase in Mg–Zn–Y alloys. Mater. Sci. Eng., A **397**, 22–34 (2005)
10. S. Sen, T. Mukerji, A generalized classical nucleation theory for rough interfaces: application in the analysis of homogeneous nucleation in silicate liquids. J. Non-Cryst. Solids **246**, 229–239 (1999)
11. F. Spaepen, A structural model for the solid-liquid interface in monatomic systems. Acta Metall. **23**, 729–743 (1975)

12. F. Shi, *Quasicrystal Phase and Its Formation Mechanism in Ordinary Solidified Mg–Zn–Y Alloy* (Xi'an University of Technology, 2003, in Chinese)
13. Z.P. Luo, S.Q. Zhang, Y.L. Tang, D.S. Zhao, On the stable quasicrystals in slowly coiled Mg-Zn-Y alloys. Scripta Metall. Mater. **32**, 1411–1416 (1995)
14. Y.B. Zhang, S. Yu, Y. Song, X. Zhu, Microstructures and mechanical properties of quasicrystal reinforced Mg matrix composites. J. Alloys Compd. **464**, 575–579 (2008)
15. H.Q. Hu, *Metal Solidification Principle* (China Machine Press, Beijing, 2000, in Chinese)